

ESTIMATION OF BACK EMF FOR PMSM AT LOW SPEED RANGE

KONRAD URBANSKI

Poznan University of Technology
Institute of Control and Information Engineering
Poznan, Poland

e-mail: konrad.urbanski@put.poznan.pl

In the paper is presented a comparison of three method of back electromotive force estimation. Presented structures: the observers and the simulator, are utilized to estimate the back electromotive force for speed range below single revolution per second. Their instantaneous values are used then to calculate the shaft position of the permanent magnets synchronous motor. Performance of such structures is very important in a case of position estimation at the low speed range. These methods are based on the following structures for back electromotive force estimation: observer for model of the electrical part of the motor, the observer with modified correction function, and estimation based on the simplified model. Obtained in this way the instantaneous values of the back electromotive force, depending on the method of obtaining them, are characterized by different quality and accuracy of the estimated shaft position. Estimated and measured values are compared and discussed.

KEYWORDS

sensorless control, permanent magnet synchronous motor (PMSM), observer, variable speed drive, vector control, back electromotive force (back EMF)

1. INTRODUCTION

The permanent magnet synchronous motor is very often used in the industry. Its main advantages are high power density, high torque-to-inertia ratio, small torque ripple and precise control at low speed range. Such features makes the PMSM the perfect solution for advanced drives. However, high efficiency and small size causes, that it can also be used in household appliances. To exploit presented advantages, a vector control should be used. In that case, a motor shaft position sensor is required to enable the effective control of a PMSM. Sensorless control of PMSM drive is still current research task. However, the method of sensorless control in the medium speed [Gao 2013] [Kim 2011] [Li 2012] [Raggl 2009] [Urbanski 2004] has been described in many publications and implementations, but in the low and zero speed range, the new solutions are still reported [Gu 2009] [Urbanski 2011]. Currently for the low and zero speed range, are introduced the additional test signals into the control chain, and the current responses determines the shaft position [Corley 1998] [Qi 2009] [Schrodl 2008]. It is assumed, that the estimation method based on back electromotive force is not suited for low speed range [Hamida 2013] [Wang 2012], since the estimated signals are distorted or noisy, so that it is hard to get the proper operation in this area in the sensorless mode.

In the research is used the structure of the drive, which is well-known vector control system (Fig. 1). Drive is equipped with cascade control structure using closed speed control loop (speed controller R_{ω}), with the inner current control loops (controllers in dq axis: R_{id} , R_{iq}).

The system is equipped with position/speed sensor (Fig. 2) which is used only to comparison purposes and analyze the position estimation quality. The estimated value of the actual motor shaft position is used in the transforming blocks of the coordinate system $dq \rightarrow \alpha\beta$ and $\alpha\beta \rightarrow dq$. The estimated value of the speed is used in control loop of the speed. Used in the investigations the control algorithm gives a possibility to change the mode of operation: drive can work in closed mode (observed values are used to control drive) or in open mode (observed values are

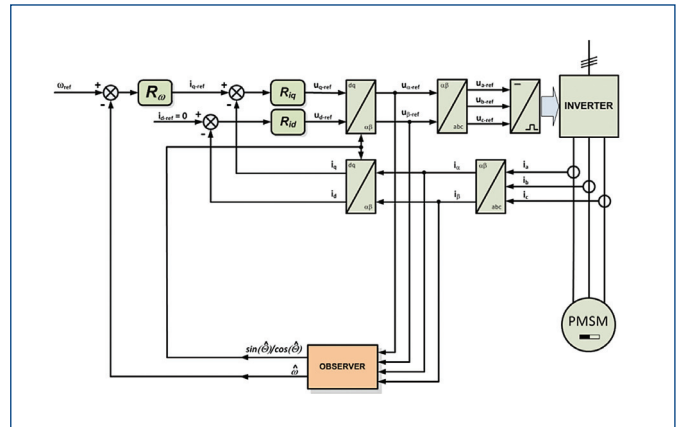


Figure 1. The sensorless drive structure used in a study

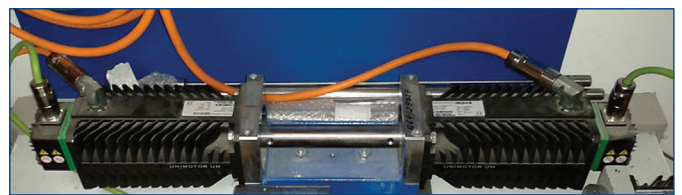


Figure 2. The laboratory stand: test and load machine

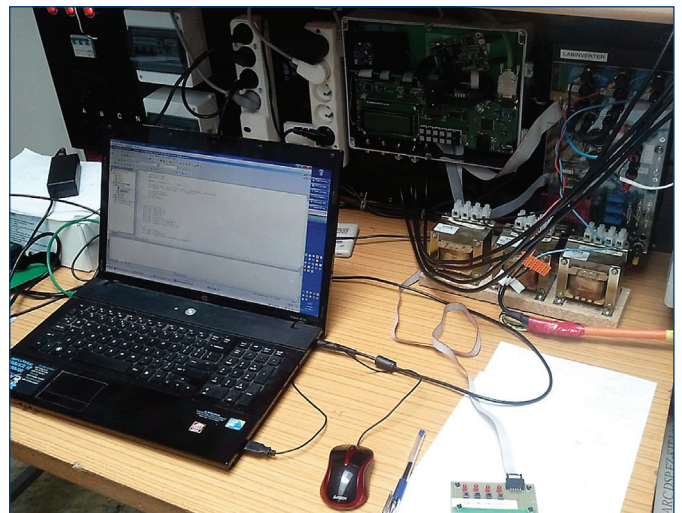


Figure 3. General view of research stand

only considered). The examined motor is fed by the laboratory inverter (Fig. 3), which works with the six pulse rectifier. Visible in Fig. 2 the second machine is fed by industrial inverter and in that case it is used only to drive the examined motor in order to record the back EMF. This machine is working also as the controlled load source (not used in these studies). The main control system is based on the floating point DSP from SHARC family. Examined drive operates using rotor oriented strategy. All structures, both controllers and estimators are calculated using a time period equal 100 ms. Inverter's carrier frequency is also equal 10 kHz. A reference voltage is used instead of measured ones in order to achieve smooth observed values. Usage of the reference voltage value in the estimation algorithm significantly facilitates calculations and affects the quality of the values obtained during shaft position calculations. The quality was defined as the low value and the small oscillations of the position error. However, such method gives significantly different values of the motor terminal voltage and the reference ones in a case of low speed range, where voltage reaches low values. Selected observer estimates the back EMFs in stationary

coordinate system $\alpha\beta$ and then calculates sine and cosine of the shaft position. Finally, the motor shaft rotational speed should be calculated to proper operation of that speed control structure.

2. MOTOR MODEL

It can be assumed that for typical simplifying assumptions, where the rotor has no windings, eddy currents and the effect of temperature are neglected and produced by the rotor the flux is constant [Vas 1998] (which, however, when working in a low speed range, at least this last assumption is too simplistic), the general form of the electrical part of the PMSM model in $\alpha\beta$ stationary orthogonal coordinates can be expressed as follows (in a case of magnetic symmetry):

$$\begin{aligned} \frac{di_{\alpha}}{dt} &= -\frac{R}{L} \cdot i_{\alpha} - \frac{1}{L} \cdot e_{\alpha} + \frac{1}{L} \cdot v_{\alpha} \\ \frac{di_{\beta}}{dt} &= -\frac{R}{L} \cdot i_{\beta} - \frac{1}{L} \cdot e_{\beta} + \frac{1}{L} \cdot v_{\beta} \end{aligned} \quad (1)$$

$$\begin{aligned} \Psi_{\alpha} &= L \cdot i_{\alpha} + \Psi_f \cdot \cos(\hat{\Theta}) \\ \Psi_{\beta} &= L \cdot i_{\beta} + \Psi_f \cdot \sin(\hat{\Theta}) \end{aligned} \quad (2)$$

and the mechanical part of the PMSM is presented as:

$$\begin{aligned} \frac{d\omega}{dt} &= \frac{1}{J} \cdot (\Psi_{\beta} \cdot i_{\alpha} - \Psi_{\alpha} \cdot i_{\beta} - T_L) \\ \frac{d\Theta}{dt} &= \omega \end{aligned} \quad (3)$$

The motor model with state variables i_{α} , i_{β} , ω and Θ is nonlinear. In a concept without mechanical sensor, the speed and shaft position will be estimated however, all state variables are measurable. The symbols i_{α} , i_{β} , Ψ_{α} , Ψ_{β} , Ψ_f , e_{α} , e_{β} are stator current, stator and magnetizing flux linkage and induced back EMF in $\alpha\beta$ coordinates. Symbols v_{α} , v_{β} are the components of input stator voltage, R and L are the stator windings resistance and inductance. The symbols ω and Θ are the rotor speed and the position, J is the moment of inertia and T_L is the load torque treated as an external disturbance. Such model formula makes easy derivation of the observer structure. Just use only the electrical part of the motor model is sufficient to develop a position observer which is working with satisfactory accuracy.

3. BACK EMF ESTIMATION METHODS

Used in the paper a method of the position estimation is based on the estimated value of the back EMF which is induced in the stator windings, and then a shaft position is calculated. Used in the study the estimation method is based mainly on a Luenberger observer [Luenberger 1971] where a proportional correction function is applied. The other method is based on the extended correction function into proportional-integral correction function. This P-I form is the results of truncation of the P-I-I² form of correction function, which may be used in a various PMSM drive

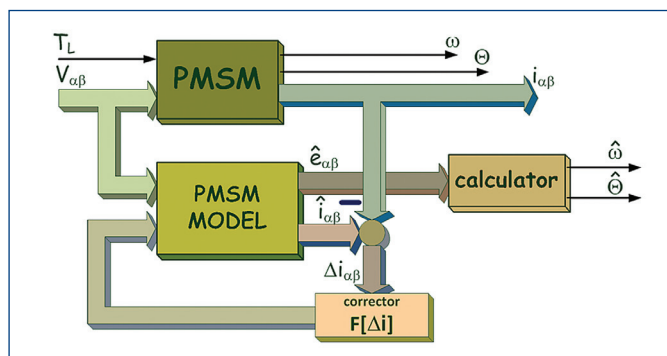


Figure 4. General structure of the back EMF observer including position and speed calculator

configurations [Urbanski 2011][Urbanski 2013]. Estimator is prepared according to (1) as a $\alpha\beta$ system. It is based on motor model described only by the two first electrical equations in stationary coordinates system $\alpha\beta$, with state variables i_{α} , i_{β} , input variables v_{α} , v_{β} (reference voltage) and back EMF e_{α} , e_{β} which may be considered as disturbances [Parasiliti 1997]. The general structure for estimation technique is presented in Fig. 4. Depending on the form of correction function, estimated back EMFs have different quality, which affect the quality of the calculated instantaneous value of the shaft position.

A: Reference Observer

As a reference a structure of Luenberger observer is used to estimation the back EMF. The basic version of observer equations set has the following form:

$$\begin{aligned} \frac{d\hat{i}_{\alpha}}{dt} &= -\frac{R}{L} \hat{i}_{\alpha} - \frac{1}{L} \hat{e}_{\alpha} + \frac{1}{L} v_{\alpha} + K_{i\alpha} (\hat{i}_{\alpha} - i_{\alpha}) \\ \frac{d\hat{i}_{\beta}}{dt} &= -\frac{R}{L} \hat{i}_{\beta} - \frac{1}{L} \hat{e}_{\beta} + \frac{1}{L} v_{\beta} + K_{i\beta} (\hat{i}_{\beta} - i_{\beta}) \\ \frac{d\hat{e}_{\alpha}}{dt} &= K_{e\alpha} (\hat{i}_{\alpha} - i_{\alpha}) \\ \frac{d\hat{e}_{\beta}}{dt} &= K_{e\beta} (\hat{i}_{\beta} - i_{\beta}) \end{aligned} \quad (4)$$

where $K_{i\alpha}$, $K_{i\beta}$ are the current correction gain and $K_{e\alpha}$, $K_{e\beta}$ are the back EMF correction gain for $\alpha\beta$ coordinate system, respectively. In that case, a correction function has a form as is used in the P-type controller. There are only two observer parameters to designate ($K_i = K_{i\alpha} = K_{i\beta}$, $K_e = K_{e\alpha} = K_{e\beta}$). Such observer is well described in other publications.

B: Observer with the Modified Correction Function

Correction function for use at low speed range may be a proportional, so the corrector is just a set of gains. In order to increase the accuracy of observation especially in dynamic states, the higher speed range or in high-step calculations, the structure of the corrector can be expanded by adding another integrator (which gives a correction function form as is used in the PI-type controller) or two additional integrators, to give correction function P-I-I² [Urbanski 2013], as is presented in matrix form:

$$F_{PII}[\Delta i] = K_p[\Delta i] + K_i \int [\Delta i] dt + K_{II} \int \left[\int [\Delta i] dt \right] dt \quad (5)$$

where K_p , K_i and K_{II} are correction factor, respectively for proportional, integral and double integral component of the observer's corrector. This correction function F (5) may be used in place the gains K in (4). At low speed range it is not necessary to use all six observer parameters as in a case of correction P-I-I², a P-I is sufficient to improve estimation quality, as is used in present study. In that case, a correction function takes the form (6):

$$F_{PI}[\Delta i] = K_p[\Delta i] + K_i \int [\Delta i] dt \quad (6)$$

and the observer equations set has the following form:

$$\begin{aligned} \frac{d\hat{i}_{\alpha}}{dt} &= -\frac{R}{L} \hat{i}_{\alpha} - \frac{1}{L} \hat{e}_{\alpha} + \frac{1}{L} v_{\alpha} + K_{i\alpha} (\hat{i}_{\alpha} - i_{\alpha}) \\ \frac{d\hat{i}_{\beta}}{dt} &= -\frac{R}{L} \hat{i}_{\beta} - \frac{1}{L} \hat{e}_{\beta} + \frac{1}{L} v_{\beta} + K_{i\beta} (\hat{i}_{\beta} - i_{\beta}) \\ \frac{d\hat{e}_{\alpha}}{dt} &= K_{e\alpha} (\hat{i}_{\alpha} - i_{\alpha}) \\ \frac{d\hat{e}_{\beta}}{dt} &= K_{e\beta} (\hat{i}_{\beta} - i_{\beta}) \end{aligned} \quad (7)$$

In assumption the symmetry of the motor in axis α and β , there are only four parameters, which should be chosen: the coefficients for the proportional part and for the integrating part, in current equations $K_{i,\alpha-P} = K_{i,\alpha-P} = K_{i,\beta-P}$, $K_{i,\alpha-I} = K_{i,\alpha-I} = K_{i,\beta-I}$ and the coefficients for the proportional part and for the integrating part, in back EMF equations $K_{e,\alpha-P} = K_{e,\alpha-P} = K_{e,\beta-P}$, $K_{e,\alpha-I} = K_{e,\alpha-I} = K_{e,\beta-I}$.

C: Simulator

In fact this is reduced structure from PMSM part, the voltage equation, in a case of elimination the inductance in the motor model. That

structure is used for comparison purposes only. There is no correction feedback hence its equation set looks so tiny:

$$\begin{aligned} \hat{e}_\alpha &= v_\alpha - i_\alpha \cdot R \\ \hat{e}_\beta &= v_\beta - i_\beta \cdot R \end{aligned} \quad (8)$$

It is assumed, that estimation of unknown state variables with the use of the simulator (defined as the appropriately transformed the model) gives a poor effects however, the estimation error is set within the certain limits due to the lack of possibility to integrate the error. The disadvantage of this structure is mainly the sensitivity on the accuracy of the estimation of object parameters. The advantage of this structure is the exceptional simplicity.

4. POSITION AND SPEED CALCULATION

After estimation the back EMF, next step is to calculate the shaft position and speed. In fact, estimation a sine and cosine of the shaft position is enough to use a vector control, no calculation of the shaft angle is needed. The equations used to calculate the position are presented below:

$$\sin(\hat{\theta}) = -\frac{\hat{e}_\alpha}{|\hat{e}|} \quad \cos(\hat{\theta}) = \frac{\hat{e}_\beta}{|\hat{e}|} \quad (9)$$

where

$$|\hat{e}| = \sqrt{\hat{e}_\alpha^2 + \hat{e}_\beta^2} \quad (10)$$

Such obtained shaft position information may be used in conversion blocks of the coordinates systems. It works perfectly, including calculation both position and speed at medium and high speed range as is shown in Fig. 5, where reference speed value was equal 157 rad/s. The measured position and position estimation error scale is tenfold different in that figure. A perfect match of the measured and estimated sine of the shaft position is visible (Fig. 5, channel 3 and 4). The other problem is a speed calculation, which should be fast and reliable especially at low speed range. In that speed range, nonlinearity in a flux distribution, a cogging torque, inverter's dead time and others phenomena have strong impact on desired motor torque, which is desired to obtain not oscillating speed waveform. It is clearly visible in Fig. 6 for drive operating in the sensor mode. Even in case a constant reference current in q axis, the measured speed is not constant (Fig. 6, channel 3). A typical equation for the speed calculation from the estimated back EMF is shown below:

$$|\hat{\omega}| = \frac{|\hat{e}|}{k_e} \quad (11)$$

where k_e is scaling factor. Such method based on the calculation the back EMF module, as the one step method is fast (there is no need to know the previous value) however, if the estimated back EMF differ significantly from a sinusoid in shape that method may fail, if used without modification [Urbanski 2014]. It is not working properly at low speed due to shape of the estimated back EMF, which is not sinusoidal even in a case if drive is operating at sensor mode. Speed calculation using (11) gives waveforms presented in Fig. 7. As was mentioned in the third section, three structures used to estimate the back EMF were examined. The marks A/B/C used in captions in the figures correspond to the structures, which were used in the third section. In the sensor mode, at steady state, the estimated speed value oscillates (Fig. 7, channel 4) what does not allow the proper operation at the sensorless mode. However, the position estimation is performed with acceptable accuracy (Fig. 7, channel 1 and 2). Despite these unfavorable phenomena, a sensorless operation has been started. For such settings of the speed controller, as the controller for the sensor based system, drive did not work. In a case of parameter set for 'slower' speed controller performance, the drive operates very poorly (Fig. 8) only for constant reference speed however, this means that one of the

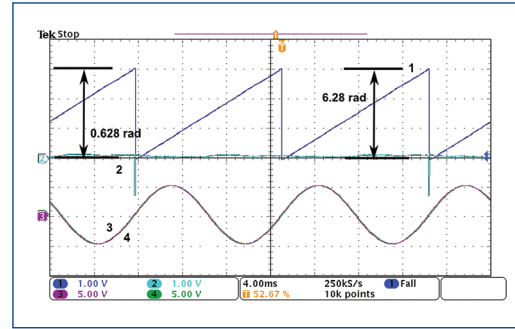


Figure 5. Medium speed, sensorless mode, structure B, time base 4 ms/div: $\omega_{ref} = 157$ rad/s, CH1: measured position, CH2: position estimation error (other scale than the CH1), CH3: sine of the measured position, CH4: sine of the estimated position

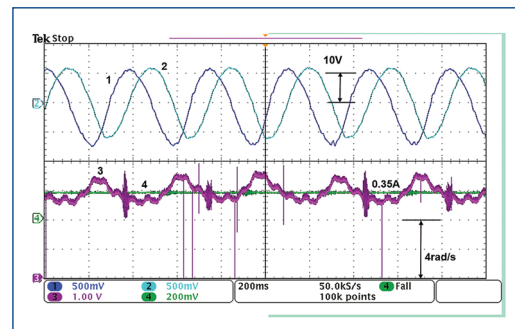


Figure 6. Low speed, sensor mode, structure B, time base 200 ms/div: constant reference current $i_q = 0.35$ A, CH1: estimated back EMF $-E_\alpha$, CH2: estimated back EMF $-E_\beta$, CH3: measured speed (average value 5 rad/s), CH4: reference current i_q

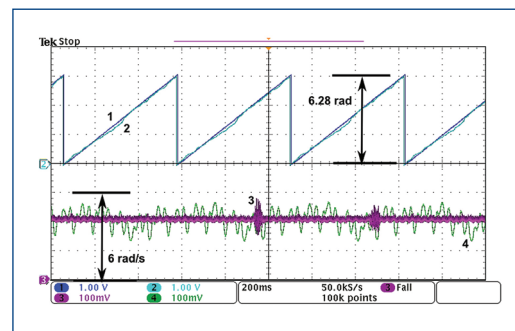


Figure 7. Low speed, sensor mode, structure A, time base 200 ms/div: $\omega_{ref} = 4$ rad/s, CH1: measured position, CH2: estimated position, CH3: measured speed, CH4: estimated speed

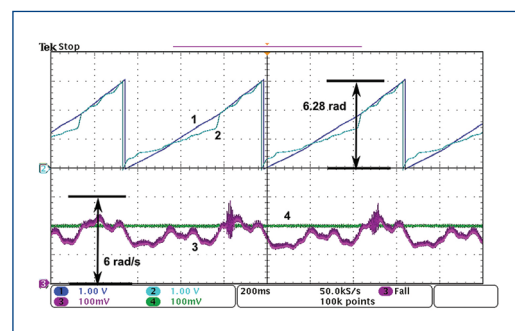


Figure 8. Low speed, sensorless mode, structure A, time base 200 ms/div: $\omega_{ref} = 4$ rad/s (average measured speed 3.27 rad/s), CH1: measured position, CH2: estimated position, CH3: measured speed, CH4: estimated speed

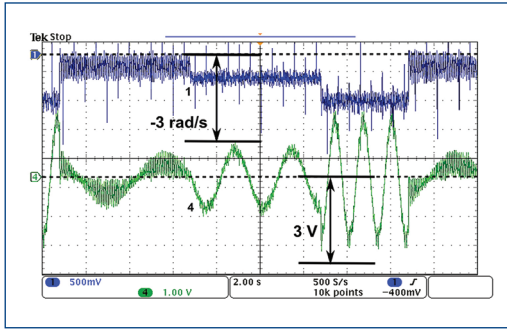


Figure 9. Low speed, sensor mode, back EMF recording, time base 2 s/div, $\omega_{ref} = 0.4 \rightarrow 0.8 \rightarrow 1.6$ rad/s, CH1: measured speed, CH4: measured back EMF – E_{BC} (motor phase connectors B-C)

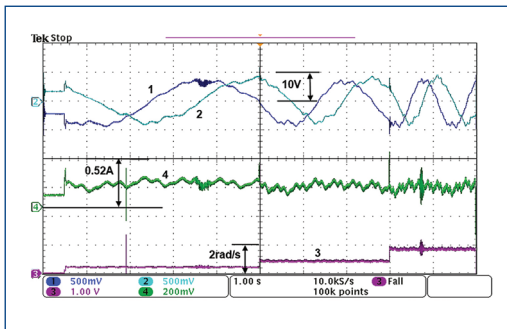


Figure 10. Low speed, sensor mode, structure A, time base 1 s/div: $\omega_{ref} = 0 \rightarrow 0.4 \rightarrow 0.8 \rightarrow 1.6$ rad/s, CH1: estimated back EMF – E_{α} , CH2: estimated back EMF – E_{β} , CH3: measured speed, CH4: measured current i_q

solution may be to use the nonlinear speed controller or compensation system e.g. just like as [Brock 2005]. At the constant torque range, the back EMF amplitude changes proportional to motor speed. The experiment confirms that this assumption is valid even at low speed range (Fig. 9). Recorded waveforms were obtained using industrial inverter after complete the autotune procedure. However, the above assumption may be improper, in a case of estimation the back EMF, at least in a case of the presented estimators. In a case the speed reaches a certain low value and below, the estimated back EMF amplitude almost ceases to change. It is visible even in a case of doubling the shaft speed, if the reference voltage is used as the input of the observer instead the measured voltage. It is clearly visible in Fig. 10. Estimated value of the back EMF obtained at low speed is not noisy or somehow damaged. However, speed change from 0.4 rad/s to 1.6 rad/s does not cause noticeable changes the back EMF amplitude (Fig. 10, channel 1 and 2). Moreover, there is no decrease to zero the back EMF vector length at standstill in a case of deceleration. This phenomenon is visible for all the estimation structures. The irregularities in the back EMF and this phenomenon eliminates the direct usage of (11) to calculate the speed however, the position estimation may work with acceptable accuracy. Lack of influence of irregularities in a back EMF waveforms on estimating the position is visible in Fig. 11, where a comparison of sine and cosine of the shaft position, and also back EMF is featured. Scale of channel (1 and 2), and also (3 and 4) has been normalized to visual comparison. The calculated position using (9) is sufficiently smooth. To maintain a constant speed value, the q axis current constantly changes its value (Fig. 10, channel 4). This indicates the need of high dynamics of the speed controller, which is a great problem for obtain the reliable sensorless operation of drive using traditional control structure. The effect of direct use (11) in order to calculate the speed, is also visible in Fig. 12. Calculated speed waveform (channel 4) oscillates, due to non-sinusoidal back EMF shape, and its average value varies slightly. In typical speed control structure, such signal is completely useless to control the machine

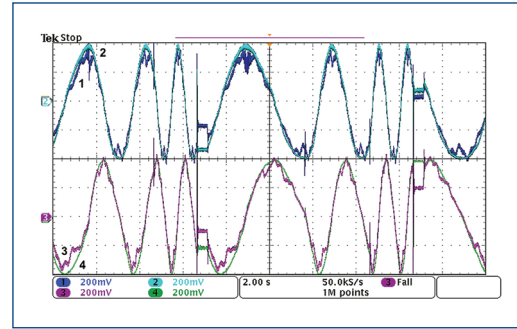


Figure 11. Low speed, sensor mode, structure A, time base 2 s/div: $\omega_{ref} = 0 \rightarrow 0.4 \rightarrow 0.8 \rightarrow 1.6$ rad/s, comparison of the instantaneous values of the estimated back EMF and the estimated shaft position, CH1: estimated back EMF – E_{α} , CH2: scaled sine of the estimated position, CH3: estimated back EMF – E_{β} , CH4: scaled cosine of the estimated position

speed. In the study have been compared the performance of the presented structures for estimation the shaft position. The following features were evaluated: noise level in the calculated sine and cosine of the shaft position, distortion in sine and cosine in a case of step change of the reference speed and the quality of the estimated back EMF vector length. All the waveforms, except those presented in Fig. 5 and Fig. 8, were obtained in the sensor mode.

The following tests were realized: cyclic change of the reference speed – (also from zero) 0.4 rad/s by 0.8 rad/s up to 1.6 rad/s, or reversal, motor unloaded. The operation of the structures A, B and C is shown in Fig. 12 Fig. 15 however, in Fig. 15 are presented waveforms for doubled the total moment of inertia. It is noticeable, that modify the correction function by additional integrators of the observer, improves

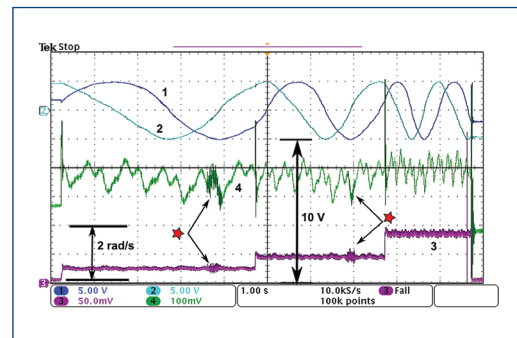


Figure 12. Low speed, sensor mode, structure A, time base 1 s/div: $\omega_{ref} = 0 \rightarrow 0.4 \rightarrow 0.8 \rightarrow 1.6$ rad/s, CH1: sine of the estimated position, CH2: cosine of the estimated position, CH3: measured speed, CH4: estimated back EMFs module

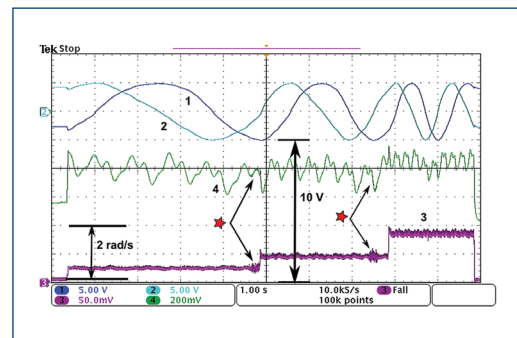


Figure 13. Low speed, sensor mode, structure B, time base 1 s/div: $\omega_{ref} = 0 \rightarrow 0.4 \rightarrow 0.8 \rightarrow 1.6$ rad/s, CH1: sine of the estimated position, CH2: cosine of the estimated position, CH3: measured speed, CH4: estimated back EMFs module

the smoothness of the calculated back EMF module (Fig. 12, Fig. 13, channel 4). More important is the significant decrease the distortion of that signal for structure B, which were visible in a case of step change of speed for structure A. The possibility to use smaller correction factors and the filtering effect of the integrators in structure B results in bigger robustness on external disturbances, whose effect is visible at measured speed waveforms (the moments of the disturbances are marked as a star).

Analyzing the waveforms for structure C in Fig. 14, first of all is visible, that the estimation quality of the back EMF (channel 4) is poor. It is full of noise and its envelope is increasing strongly with increasing motor speed. Poor quality of back EMF results in low quality of calculated position (Fig. 14, channel 1 and 2). It can be seen that there are lot of interferences, which are visible in the waveforms of calculated sine and cosine. This phenomenon can not be seen in a case of using the observer (structure A or B). Doubling of the total moment of inertia does not affect noticeably the position estimation quality (Fig. 15).

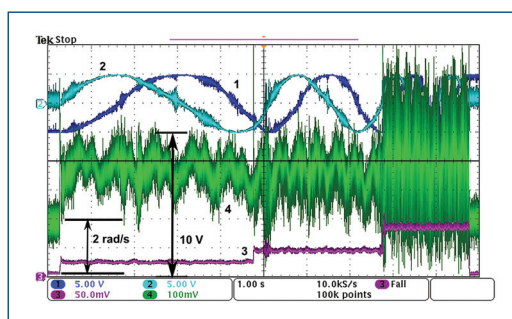


Figure 14. Low speed, sensor mode, structure C, time base 1 s/div: $\omega_{ref} = 0 \rightarrow 0.4 \rightarrow 0.8 \rightarrow 1.6$ rad/s, CH1: sine of the estimated position, CH2: cosine of the estimated position, CH3: measured speed, CH4: estimated back EMFs module

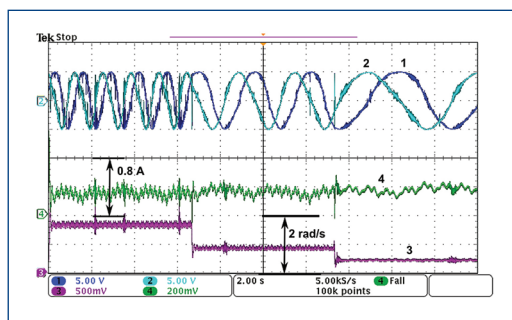


Figure 15. Low speed, sensor mode, structure C, time base 2 s/div: $\omega_{ref} = 1.6 \rightarrow 0.8 \rightarrow 0.4$ rad/s, CH1: sine of the estimated position, CH2: cosine of the estimated position, CH3: measured speed, CH4: measured current i_q , doubled the total moment of inertia

5. CONCLUSIONS

Presented results of the study on the back EMF estimation, motivates to further research on this task. Based on the presented waveforms one can concluded, that those methods allows the estimation of the motor shaft position also in the low speed range. The main question is how deep one can go down with the speed, retaining the proper position estimation using method based on back EMF estimation. The problem is especially how to extract the speed signal from such position signal. Such drive may work at sensorless mode provided that reference torque will be calculated properly. It means the necessity of work without speed feedback or the use more effective method of calculating the speed. Even in a case of speed control using sensor mode, it is hard to maintain smooth speed waveforms when using typical linear

controller, what is visible on recorded back EMF waveform (Fig. 9). Torque pulsation in PMSM affects the speed waveform in the sensorless mode especially at low speed range. It is important phenomena and should be included in control scheme to obtain the smooth speed waveform. The estimation of the back EMF (and also the position) using both structures A and B enables the sensorless operation at low speed range however, the additional integrators in structure B gives as a result better performance in rapid transients of speed and bigger robustness on electromagnetic disturbances. In a case of deceleration, estimated back EMF maintains a non-zero value at standstill. The method based on the simulator is sensitive on the accuracy of the motor resistance estimation, hence the estimation accuracy using estimator may vary, e.g. during heating the motor.

Appendix

The parameters of the motor used in experiments are:

- rated power – 1.23 kW
- nominal speed – 3000 rpm
- rated torque – 3.9 N·m
- number of poles – 6
- measured resistance – 2Ω
- measured inductance – 5.7 mH
- total moment of inertia – 24.96 kg·cm²

REFERENCES

- [Brock 2005] Brock, S. and Deskur, J. A Practical Approach to Compensation of Torque Ripple in High-Precision Permanent Magnet Motor Drives. In: International Conference on Electrical Drives and Power Electronics. Dubrovnik, Croatia, 2005
- [Corley 1998] Corley, M. J. and Lorenz, R.D. Rotor position and velocity estimation for a salient-pole permanent magnet synchronous machine at standstill and high speeds. In: IEEE Transactions on Industry Applications vol. 34 (1998), Nr. 4, 784–789
- [Gao 2013] Gao, W. and Guo, Z. Speed Sensorless Control of PMSM using Model Reference Adaptive System and RBFN. In: Journal of Networks vol. 8 (2013), Nr. 1
- [Gu 2009] Gu, S. M. et al. Study on Extend Kalman Filter at Low Speed in Sensorless PMSM Drives. In: International Conference on Electronic Computer Technology, 2009, ISBN 978-0-7695-3559-3, 311–316
- [Hamida 2013] Hamida, M.A. et al. An Adaptive Interconnected Observer for Sensorless Control of PM Synchronous Motors With Online Parameter Identification. In: IEEE Transactions on Industrial Electronics vol. 60 (2013), Nr. 2, 739–748
- [Kim 2011] Kim, H. et al. A High-Speed Sliding-Mode Observer for the Sensorless Speed Control of a PMSM. In: IEEE Transactions on Industrial Electronics vol. 58 (2011), Nr. 9, 4069–4077
- [Li 2012] Li, L. et al. Sensorless Control of PMSM Based on State Observer and the Parameter Error Analysis. In: 2012 IEEE International Conference on Power Electronics, Drives and Energy Systems (PEDES), 2012, 1–8
- [Luenberger 1971] Luenberger, D. An Introduction to Observers. In: IEEE Transactions on Automatic Control vol. 16 (1971), Nr. 6, 596–602
- [Parasiliti 1997] Parasiliti, F. et al. Sensorless Speed Control of a PM Synchronous Motor by Sliding Mode Observer. In: Industrial Electronics, 1997, ISIE'97, Proceedings of the IEEE International Symposium on, 1997, 1106–1111
- [Qi 2009] Qi, X. et al. Rotor position estimation for a sensorless PMSM using high-frequency signal injection method. In: IEEE Youth Conference on Information, Computing and Telecommunication, 2009. YC-ICT '09: IEEE, 2009 — ISBN 978-1-4244-5074-9, 54–57
- [Raggl 2009] Raggl, K. et al. Robust Angle-Sensorless Control of a PMSM Bearingless Pump. In: IEEE Transactions on Industrial Electronics vol. 56 (2009), Nr. 6, 2076–2085
- [Schrodl 2008] Schrodl, M. and Simetzberger, C. Sensorless Control of PM Synchronous Motors Using a Predictive Current Controller with

Integrated INFORM and EMF Evaluation. In: Power Electronics and Motion Control Conference, 2008. EPE-PEMC 2008. 13th: IEEE, 2008 – ISBN 978-1-4244-1741-4, 2275–2282

[Urbanski 2004] Urbanski, K. and Zawirski, K. Adaptive Observer of Rotor Speed and Position for PMSM Sensorless Control System. In: COMPEL: The International Journal for Computation and Mathematics in Electrical and Electronic Engineering vol. 23 (2004), Nr. 4, 1129–1145

[Urbanski 2011] Urbanski, K. Sensorless control of PMSM high dynamic drive at low speed range. In: 2011 IEEE International Symposium on Industrial Electronics (ISIE): IEEE, 2011 – ISBN 978-1-4244-9310-4, 728–732

[Urbanski 2013] Urbanski, K. Sensorless control of PMSM fed through the sinusoidal filter. In: 2013 15th European Conference on Power Electronics and Applications (EPE). Lille, France, 2013

[Urbanski 2014] Urbanski, K. Sensorless speed control of PMSM drive for low speed range using back EMF estimation. In: XXIII

Symposium Electromagnetic Phenomena in Nonlinear Circuits. Pilsen, Czech Republic, 2014, 47–48

[Vas 1998] Vas, P. Sensorless Vector and Direct Torque Control, Monographs in electrical and electronic engineering. Oxford; New York: Oxford University Press, 1998 – ISBN 0198564651

[Wang 2012] Wang, Z. et al. Investigation of PMSM Back-EMF Using Sensorless Control with Parameter Variations and Measurement Errors. In: Przegląd Elektrotechniczny vol. 88 (2012), Nr. 8, 182–186

CONTACT

Konrad Urbanski Ph.D.

Poznan University of Technology

Institute of Control and Information Engineering

ul. Piotrowo 3A, Poznan, 61-138, Poland

tel.: +48 61 665 28 10

e-mail: konrad.urbanski@put.poznan.pl